Experiments of Drops Impacting a Smooth Solid Surface: A Model of the Critical Impact Speed for Drop Splashing

Guillaume Riboux and José Manuel Gordillo*
Área de Mecánica de Fluidos, Departamento de Ingeniería Aeroespacial y Mecánica de Fluidos, Universidad de Sevilla, Avenida de los Descubrimientos s/n, 41092 Sevilla, Spain
(Received 20 December 2013; published 11 July 2014)

Making use of experimental and theoretical considerations, in this Letter we deduce a criterion to determine the critical velocity for which a drop impacting a smooth dry surface either spreads over the substrate or disintegrates into smaller droplets. The derived equation, which expresses the splash threshold velocity as a function of the material properties of the two fluids involved, the drop radius, and the mean free path of the molecules composing the surrounding gaseous atmosphere, has been thoroughly validated experimentally at normal atmospheric conditions using eight different liquids with viscosities ranging from $\mu = 3 \times 10^{-4}$ to $\mu = 10^{-2}$ Pa s, and interfacial tension coefficients varying between $\sigma = 17$ and $\sigma = 72$ mN m^{-1}. Our predictions are also in fair agreement with the measured critical speed of drops impacting in different gases at reduced pressures given by Xu *et al.* [Phys. Rev. Lett. 94, 184505 (2005).].

DOI: 10.1103/PhysRevLett.113.024507 PACS numbers: 47.15.km, 47.55.D-, 47.55.np

The collision of a drop against a solid surface is ubiquitous in nature and is present in a myriad of technological and scientific fields comprising ink-jet printing, combustion, or surface coating [1–3]. Given the physical properties of both the liquid and the gas, the atmospheric pressure [1], the size of the drop, and the physicochemical properties of the substrate [4], experience reveals that there exists a critical impact velocity below which the liquid simply spreads over the surface and above which the original liquid volume fragments into tiny droplets violently ejected outwards, creating what is known as a splash (see Fig. 1). In spite of the number of advances on the subject [1,5–14], a precise description of the critical conditions leading to drop splashing, is still lacking [15,16]. Indeed, the well-known equation deduced twenty years ago by Mundo *et al.* [5,11,17], as well as many empirical correlations [14], provide expressions for the critical velocity which depend only on the material properties of the liquid, and do not take into account that splashing is largely affected by the gaseous atmosphere [1]. In this Letter, we provide a theoretical framework which is consistent with our own experimental data and also with *all* previous findings.

To elucidate the precise conditions under which a drop hitting a solid surface splashes or not, we perform experiments with millimetric drops of radii R formed quasistatically at normal atmospheric conditions. Eight different liquids are slowly injected through hypodermic needles of different diameters. Drops generated in this way are spherical and fall under the action of gravity onto a dry glass slide, with a composition such that the liquids, whose physical properties are listed in Table 1 of the Supplemental Material [18], partially wet the substrate with a static contact angle ~20°. The impact speed V is varied by fixing the vertical distance between the exit of the needles and the impactor. To simultaneously record the impact process from the side with two different optical magnifications and acquisition rates, two high speed cameras focusing the impact region are placed perpendicularly to each other.

Figure 1 shows the detailed sequence of events recorded from the instant $T = 0$ at which the drop first contacts the solid. These images reveal that, initially, the drop deforms axisymmetrically, with $A(T)$ the radius of the circular wetted area [Figs. 1(a)–1(b)] and that an air bubble is entrapped at the center of the drop [3,19]; however, the

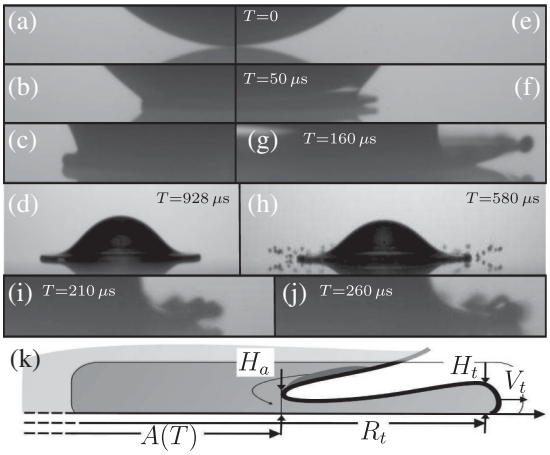

FIG. 1. (a)–(h) Sequence of events after the impact of an ethanol droplet of radius $R = 1.04$ mm for three different impact velocities, $V = 1.29$ m s^{-1} [(a)–(d), left], $V = 2.28$ m s^{-1} [(e)–(h), right], and $V = 2.01$ m s^{-1}, (i)–(j). The splash threshold velocity corresponding to these experiments is $V = 2.19$ m s^{-1}. The times in (a)–(c) are identical to those corresponding to images (e)–(g). The sketch in Fig. 1(k) illustrates the definition of the main variables used within the Letter.

presence of this tiny bubble does not affect the splash process. Figure 1(c) illustrates that for $T \geq T_e$, a thin sheet of liquid starts to be expelled from the radial position where the drop contacts the solid, i.e., $A(T_e)$, with T_e the ejection time. Of special relevance for the purposes of this study is to observe the change of trajectory experienced by the edge of the sheet as the impact velocity increases. Indeed, for the smallest values of V [Figs. 1(a)–1(d)], the lamella spreads tangentially along the solid but, for a range of larger impact velocities, the liquid initially dewets the substrate and contacts the substrate again [Figs. 1(i)–1(j)]. For even higher values of V, the front of the lamella dewets the solid [Figs. 1(f)–1(g)] and drops are finally ejected radially outwards [Figs. 1(g)–1(h)] in a way similar to the experiments reported in [20–22]. Therefore, the analysis of the images in Fig. 1 reveals that, for a splash of the type illustrated in Figs. 1(e)–1(h) to take place, two conditions need to be fulfilled simultaneously: the liquid must dewet the solid and the vertical velocity imparted to the front part of the lamella needs to be large enough to avoid the liquid to contact the solid again. To obtain a splash criterion, it is essential to observe from Figs. 1(i)–1(j) and the movies in the Supplemental Material [18], that the rewetting is a consequence of the radial growth of the liquid sheet edge, caused by capillary retraction. Throughout the Letter, times, velocities, and pressures are made dimensionless using R, V, R/V, ρV^2 as the characteristic length, velocity, time, and pressure, with ρ the liquid density and lower-case letters denoting dimensionless variables (e.g., $h_t = H_t/R$, $v_t = V_t/V$); the subscript g will be used to denote gas quantities. Next, the instant T_e at which the lamella is ejected, as well as its initial height and velocity, H_t and V_t, respectively [see Fig. 1(k)], will be calculated.

Splashing occurs when the values of both the Weber and Reynolds numbers are such that $\mathrm{We} = \rho V^2 R/\sigma \gg 1$, $\mathrm{Re} = \rho V R/\mu \gg 1$, with the dimensionless numbers We and Re measuring the relative importance of inertial and surface tension stresses (We) and inertial and viscous stresses (Re). Consequently, during the characteristic impact time R/V viscous effects are confined to thin boundary layers of typical width $\sim R\mathrm{Re}^{-1/2} \ll R$ [23], a fact suggesting that the use of potential flow theory [24,25], which neglects liquid viscosity, is appropriate to describe the liquid flow at the scale of the liquid drop. For the sake of clarity, we report here only the main results of the analysis, with further details provided in the Supplemental Material [18], where using Wagner's theory [24] we deduce that the radius of the wetted region evolves in time as $a(t) = \sqrt{3t}$ [26]. Potential flow theory also predicts that, as a consequence of the sudden inertial deceleration of the liquid when it hits the wall, a flux of momentum is directed tangentially along the substrate [22], giving rise to the ejection of a fast liquid sheet, like the one depicted in Figs. 1(c) and 1(f)–1(g). The application of the Euler–Bernoulli equation at the drop's interface, where the pressure remains constant, in a frame of reference moving at a velocity $\dot{a}$ [see Fig. 1(k)], yields that fluid particles are ejected from $a(t)$ at a speed relative to that of the ground given by $v_a = 2\dot{a} = \sqrt{3/t}$. Moreover, since the flux of tangential momentum per unit length is $\propto \rho V^2 R a(t)$ [22], [27], we thus conclude that the height h_a of the lamella at the intersection with the spreading drop, i.e., at the radial position $r = a(t)$, is $\rho V^2 R \dot{a}^2 h_a \propto \rho V^2 R a \Rightarrow h_a \propto a/\dot{a}^2 \propto t^{3/2}$, with dots denoting time derivatives [28–30].

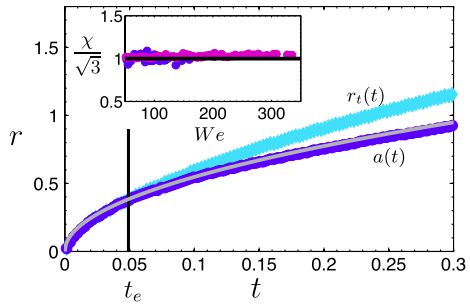

FIG. 2 (color online). Experimental radius of the wetted area compared with $a = \sqrt{3t}$ (thin solid line) for We = 98, Re = 3462 (water drop). The experimental radial position of the ejecta sheet, r_t, is also represented for times $t \geq t_e$, with t_e the ejection time. The inset represents the ratio $\chi/\sqrt{3} \simeq 1$, where χ is the coefficient obtained from the best fit of a function of the type $a = \chi\sqrt{t}$ to the experimentally measured radius $a(t)$, for a large range of Weber numbers and two different liquids: water (blue dots, $\mu \simeq 0.9$ cP, $\sigma \simeq 67.5$ mN m^{-1}) and a silicon oil (purple dots) of viscosity $\mu = 10$ cP and surface tension $\sigma \simeq 19.5$ mN m^{-1}. The ratio $\chi/\sqrt{3} \simeq 1$ also for the rest of the fluids investigated.

Figure 2 shows that the measured radius of the wetted area perfectly matches $a = \sqrt{3t}$ for all the different impact events and fluids considered, a result that fully validates our potential flow calculation. However, while our experimental evidence indicates that the ejecta sheet is only produced for $t \geq t_e$, the potential flow approach predicts the generation of a lamella for $t \geq 0$ of vanishingly small thickness $h_a \propto t^{3/2}$ with fluid velocity diverging as $v_a \propto t^{-1/2}$.

To understand the differences between potential flow results and observations note first that, in analogy with the cases of bubbles bursting at a free interface [31] and Worthington jets [32,33], the fluid feeding the lamella comes from a region where shear stresses are negligible, namely, a very narrow boundary straddling the drop's interface [dark shaded region in panel 1(k)], and not from the boundary layer growing from the stagnation point located at the axis of symmetry.

Fast fluid particles entering the liquid sheet are rapidly decelerated within the lamella due to the combined action of both the viscous shear stresses diffusing from the wall and capillary pressure. The characteristic dimensionless thickness δ of the region affected by viscous stresses at a distance $\sim h_a \ll 1$ downstream of the jet root [see Fig. 1(k)], which is the region where the jet meets the drop, is $\delta/h_a \sim 1$ (see Supplemental Material [18]). The

deceleration, provokes the fluid to accumulate at the edge of the liquid sheet and, consequently, $h_t > h_a$ [see Fig. 1(k)].

To determine t_e, note from Fig. 2 that, although the velocities of fluid particles entering the jet are $v_a = 2\dot{a} > \dot{a}$, both $a(t)$ and r_t are tangent to each other at the instant of ejection, namely, $v_t = \dot{a}$ at $t = t_e$. Thus, since the lamella can only be ejected if its tip advances faster than the radius of the wetted area, the condition for sheet ejection is $Dv/Dt = -\partial p/\partial x + \mathrm{Re}^{-1}\nabla^2 v \geq \ddot{a}$ at $t = t_e$. Here, $Dv/Dt < 0$ is the dimensionless acceleration of the material points in the sheet given by the momentum equation, p denotes pressure, and x measures the distance from the jet root. To determine t_e, since $\delta \sim h_t$, $\nabla^2 v \sim \dot{a}/h_t^2 \propto t_e^{-1/2}/h_t^2$; moreover, the increment of pressure experienced by fluid particles flowing into the edge of the lamella is the capillary pressure We^{-1}/h_t and, thus, $\partial p/\partial x \sim \mathrm{Re}^{-2}\mathrm{Oh}^{-2}/h_t^2$ with $\Delta x \sim h_t$ and $\mathrm{Oh} = \mu/\sqrt{\rho R\sigma} = \sqrt{\mathrm{We}}/\mathrm{Re}$ the Ohnesorge number. Therefore, the critical condition for sheet ejection $Dv/Dt = \ddot{a} \propto t_e^{-3/2}$ reads

$$c_1 \mathrm{Re}^{-1} t_e^{-1/2} + \mathrm{Re}^{-2}\mathrm{Oh}^{-2} = \ddot{a} h_t^2 = c^2 t_e^{3/2}, \qquad (1)$$

where we set $c_1 = \sqrt{3}/2$ for simplicity and $c = 1.1$ accounts for the proportionality constant in $h_t \propto h_a \propto t_e^{3/2}$. Figure 3(a), illustrates that Eq. (1) very well approximates the experimental results. Experiments also validate the high-Oh and low-Oh limits of Eq. (1), respectively, given by $\mathrm{Re}^{-1} t_e^{-1/2} \propto t_e^{3/2} \Rightarrow t_e \propto \mathrm{Re}^{-1/2}$ and $\mathrm{Re}^{-2}\mathrm{Oh}^{-2} \propto t_e^{3/2} \Rightarrow t_e \propto \mathrm{Re}^{-4/3}\mathrm{Oh}^{-4/3}$. Equation (1) as well as Fig. 3(a) also reveal that, for a fixed value of Oh, there is a crossover Reynolds number, Re_c, above which t_e is mostly determined by the viscous deceleration of the sheet edge, $t_e \propto \mathrm{Re}^{-1/2}$, and below which it is dominated by the capillary deceleration, $t_e \propto \mathrm{Re}^{-4/3}\mathrm{Oh}^{-4/3}$. The value of Re_c comes from equating these two limits, $\mathrm{Re}_c^{-1/2} \propto \mathrm{Re}_c^{-4/3}\mathrm{Oh}^{-4/3} \Rightarrow \mathrm{Re}_c \propto \mathrm{Oh}^{-8/5}$. In addition, Fig. 3(b) reveals that, $v_t \propto t_e^{-1/2}$ and $h_t \propto t_e^{3/2}$, providing further support to our theory.

Now, following the ideas in [4,15], we have calculated the capillary number Ca^* defined using the value of V_t at the splash transition. In Duez *et al.* [4], Ca^* is constant for the case of wetting surfaces and low viscosity liquids because, in their case, the splash and dewetting transitions coincide. However, we show in the Supplemental Material [18] that, since dewetting is a necessary but not sufficient condition for drop splashing in our case [see Figs. 1(i)–1(j)], (i) Ca^* varies appreciably with the liquid properties and (ii) Ca^* is larger than the critical capillary number Ca_d^* above which the liquid dewets the substrate. Indeed, the type of lubrication equations in [34] representing a static force balance in the direction tangent to the wall, are integrated to determine Ca_d^* (see the Supplemental Material [18] for details) and the result, particularized for $\mu = 5$ cP, reveals that Ca^* is well above Ca_d^*.

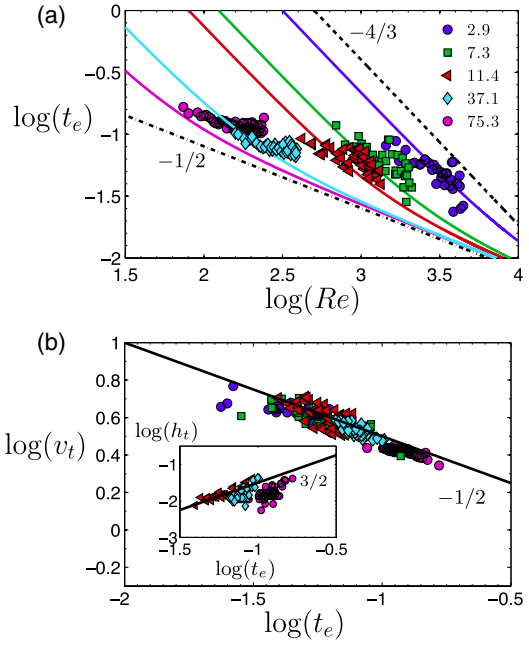

FIG. 3 (color online). (a) Comparison between the experimentally measured value of the ejection time, and the one calculated solving Eq. (1). Each of the solid lines represents the different theoretical results for different Ohnesorge numbers. The values of $1000 \times \mathrm{Oh}$, are represented in the legend. The experimentally determined ejection time is very well approximated by the solution of Eq. (1) and clearly follow the low and high Ohnesorge number limits of this equation deduced in the main text. (b) The measured experimental data follow our predictions for both v_t and h_t.

Thus, to determine the critical speed of an impacting drop, we note first that splashing occurs as a consequence of the vertical lift force ℓ, imparted by the gas on the edge of the liquid sheet. The lift force results from the addition of two contributions: the lubrication force $\sim K_l \mu_g V_t$ and the suction force $\sim K_u \rho_g V_t^2 H_t$. The former is exerted at the wedge formed between the substrate and the edge of the lamella, and the latter, at the top part of it [see Fig. 4(a)]. In the Supplemental Material [18] we show that $K_l \simeq -[6/\tan^2(\alpha)][\ln(19.2\lambda/H_t) - \ln(1 + 19.2\lambda/H_t)]$, with λ the mean free path of gas molecules, α the wedge angle which, for the case of partially wetting solids considered here does not seem to significatively depend on liquid viscosity [35], and $K_u \simeq 0.3$. Since the local gas Reynolds number based on H_t and V_t is $\sim O(10)$, both the viscous and inertial contributions to the lift force need to be taken into account (see the Supplemental Material [18] for details). Therefore, the vertical force balance per unit length, when applied at the edge of the lamella, reads $\rho H_t^2 \dot{V}_v \sim \ell$ with V_v the vertical velocity, whose characteristic value at the instant when the liquid front has raised a distance $\sim H_t$ above the substrate is given by

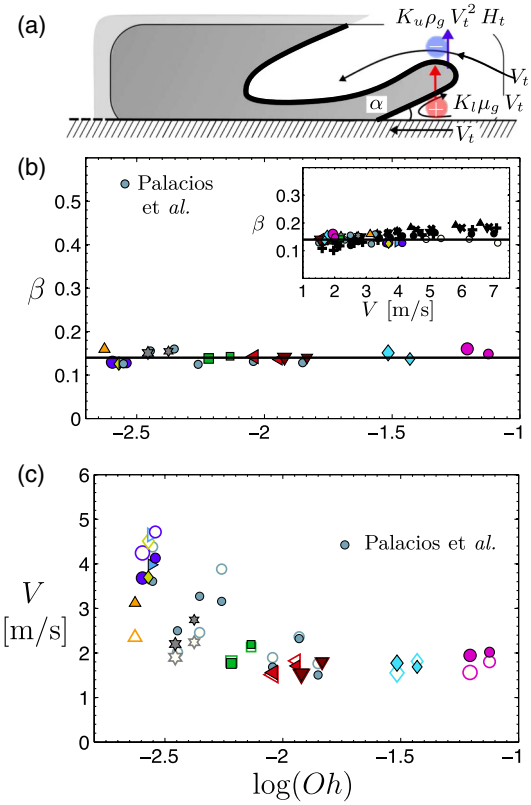

FIG. 4 (color online). (a) The total lift force arises as the addition of the force in the wedge of angle α and the force at the top part of the lamella. The plus (minus) signs indicate the regions where the gauge pressure is positive (negative). (b) Values of the function β calculated through Eq. (4) for the different liquids and drop diameters investigated. Experimental data from [14] have also been included. The inset shows that the splash threshold velocity V corresponding to the experiments in Xu, Zhang, and Nagel [1] (black symbols, with the same meaning as in this reference) is also characterized by $\beta \simeq 0.14$. Our own data, as well as those in [14] are also included in the inset. (c) The open symbols represent the splash threshold velocities predicted by the solution of Eqs. (1) and (4) with $\beta \simeq 0.14$, while the experimental data points are represented using solid symbols.

$$V_v \sim \sqrt{\ell/(\rho H_t)} \quad \text{where} \quad \ell = K_l\mu_g V_t + K_u\rho_g V_t^2 H_t. \tag{2}$$

For the edge of the sheet not to contact the solid again [see Figs. 1(i)–1(j)], V_v needs to be larger than $\dot{R}_c$. Here, R_c is the rim radius of curvature which, once the liquid dewets the substrate, grows in time as a consequence of capillary retraction. Naming V_r the well-known Taylor-Culick velocity given by the momentum balance $2\sigma = \rho V_r^2 H_t$,

$$V_r = \sqrt{2\sigma/\rho H_t}, \tag{3}$$

and inserting this result into the mass balance $dR_c^2/dT \sim V_r H_t$, one readily obtains that, at the instant when the liquid separates from the substrate, for which $R_c \simeq H_t/2$, $\dot{R}_c \sim V_r$. Hence, the splash threshold condition reads $\beta = V_v/V_r \propto (\ell/\sigma)^{1/2} \sim O(1)$, with V_v and V_r, respectively, given in Eqs. (2)–(3). Using the expression for the lift force ℓ in Eq. (2), the splash condition can thus be expressed as

$$\beta = \left(\frac{K_l\mu_g V_t + K_u\rho_g V_t^2 H_t}{\sigma}\right)^{1/2} \sim O(1). \tag{4}$$

To check the validity of Eq. (4), Eq. (1) is used first to calculate the ejection time $t_{e,\mathrm{crit}}$ corresponding to the values of We, Re, ρ/ρ_g, and μ/μ_g for which the splash transition is experimentally observed. Once $t_{e,\mathrm{crit}}$ is known, $V_t = \sqrt{3}/2 V t_{e,\mathrm{crit}}^{-1/2}$, $H_t = 2.8R\sqrt{12}/\pi t_{e,\mathrm{crit}}^{3/2}$ and β is determined through Eq. (4). Figure 4(b) demonstrates that the splash threshold is characterized by a nearly constant value of β, independent of the type of liquid considered, as predicted by Eq. (4). The open symbols in Fig. 4(c), representing the splash threshold velocities calculated solving Eq.s (1) and (4) for $\beta \simeq 0.14$, are fairly close to those measured experimentally, a fact further supporting our theory. Interestingly enough, the inset in Fig. 4(b) shows that the splash threshold corresponding to all the experimental data in Xu *et al.* [1], where the critical speed of drops of different liquids falling within several gases and different pressures is investigated, is also characterized by $\beta \simeq 0.14$.

Since the lift force ℓ is dominated by the contribution coming from the overpressures in the wedge, $\ell \sim K_l\mu_g V_t$ (see the Supplemental Material [18] for details) and K_l is approximately constant because of its logarithmic dependence on the physical parameters, the splash criterion (4) at normal atmospheric conditions can be approximated by $(\mu_g V/\sigma) t_{e,\mathrm{crit}}^{-1/2} \propto C$, with $t_{e,\mathrm{crit}}$ the solution of Eq. (1) and C a constant. Because of the fact that $t_{e,\mathrm{crit}} \propto \mathrm{Re}^{-4/3}\mathrm{Oh}^{-4/3}$ [see Fig. 3(a)] in the low-Oh limit, the previous approximate criterion results in $\mathrm{Oh}_g\mathrm{Oh}^{5/3}\mathrm{Re}^{5/3} \equiv (\mathrm{Re}\,\mathrm{Oh}_g^{8/5})^{5/3}(\mu/\mu_g)^{5/3} \propto C'$, where $\mathrm{Oh}_g = \mu_g/\sqrt{\rho R\sigma}$. In the high-Oh limit, $t_{e,\mathrm{crit}} \propto \mathrm{Re}^{-1/2}$ [see Fig. 3(a)] and, in this case, the approximate splash criterion is $\mathrm{Oh}_g\mathrm{OhRe}^{5/4} \equiv (\mathrm{Re}\,\mathrm{Oh}_g^{8/5})^{5/4}(\mu/\mu_g) \propto C''$. These power law expressions are experimentally validated in the Supplemental Material [18], giving a physical explanation to the well-known correlation by Mundo *et al.* [5,14,15] and to the interesting finding in [36] that the splash threshold condition cannot be solely characterized in terms of Oh and Re. Let us emphasize that these power law expressions are simply approximations to our theory, expressed by Eqs. (1) and (4).

To conclude, we have deduced a criterion expressing the splash threshold velocity of a drop impacting on a smooth, dry surface as a function of the liquid density and viscosity, the millimetric drop radius, the gas density and viscosity,

the interfacial tension coefficient, and the nanometric mean free path of gas molecules.

The authors wish to express their most sincere gratitude to Professor A. Korobkin for useful suggestions. Comments by A. Sevilla, J. Rodríguez-Rodríguez, and D. van der Meer as well as Alonso Fernández for the numerical values of K_u, are also acknowledged. This work has been supported by the Spanish MINECO under Project No. DPI2011-28356-C03-01, partly financed with European funds.

*jgordill@us.es

[1] L. Xu, W. W. Zhang, and S. R. Nagel, Phys. Rev. Lett. **94**, 184505 (2005).
[2] V. Bergeron, D. Bonn, J. Martin, and L. Vovelle, Nature (London) **405**, 772 (2000).
[3] W. Bouwhuis, R. C. A. van der Veen, T. Tran, D. L. Keij, K. G. Winkels, I. R. Peters, D. van der Meer, C. Sun, J. H. Snoeijer, and D. Lohse, Phys. Rev. Lett. **109**, 264501 (2012).
[4] C. Duez, C. Ybert, C. Clanet, and L. Bocquet, Nat. Phys. **3**, 180 (2007).
[5] C. Mundo, M. Sommerfeld, and C. Tropea, Int. J. Multiphase Flow **21**, 151 (1995).
[6] S. Mandre, M. Mani, and M. P. Brenner, Phys. Rev. Lett. **102**, 134502 (2009).
[7] L. Duchemin and C. Josserand, Phys. Fluids **23**, 091701 (2011).
[8] A. Latka, A. Strandburg-Peshkin, M. M. Driscoll, C. S. Stevens, and S. R. Nagel, Phys. Rev. Lett. **109**, 054501 (2012).
[9] J. M. Kolinski, S. M. Rubinstein, S. Mandre, M. P. Brenner, D. A. Weitz, and L. Mahadevan, Phys. Rev. Lett. **108**, 074503 (2012).
[10] C. Josserand and S. Zaleski, Phys. Fluids **15**, 1650 (2003).
[11] J. Bird, S. Tsai, and H. Stone, New J. Phys. **11**, 063017 (2009).
[12] R. Rioboo, M. Marengo, and C. Tropea, Exp. Fluids **33**, 112 (2002).
[13] A. Yarin, Annu. Rev. Fluid Mech. **38**, 159 (2006).
[14] J. Palacios, J. Hernandez, P. Gomez, C. Zanzi, and J. Lopez, Exp. Therm. Fluid. Sci. **44**, 571 (2013).
[15] M. Rein and J.-P. Delplanque, Acta Mech. **201**, 105 (2008).
[16] J. Snoeijer and B. Andreotti, Annu. Rev. Fluid Mech. **45**, 269 (2013).
[17] S. T. Thoroddsen, M. J. Thoraval, K. Takehara, and T. G. Etoh, Phys. Rev. Lett. **106**, 034501 (2011).
[18] See Supplemental Material at http://link.aps.org/supplemental/10.1103/PhysRevLett.113.024507 for physical properties of the fluid used, for a comparison of our theory with other experimental data and widely used experimental correlations and for the mathematical derivations of: i) the potential flow expressions used along the text, ii) the critical capillary number for the dewetting transition and iii) the expressions of K_l and K_u.
[19] S. Thoroddsen, T. Etoh, T. K., N. Ootsuka, and Y. Hatsuki, J. Fluid Mech. **545**, 203 (2005).
[20] S. Thoroddsen, J. Fluid Mech. **451**, 373 (2002).
[21] E. Villermaux and B. Bossa, J. Fluid Mech. **668**, 412 (2011).
[22] I. Peters, D. van der Meer, and J. M. Gordillo, J. Fluid Mech. **724**, 553 (2013).
[23] H. Schlichting, *Boundary-Layer Theory* (McGraw-Hill, New York, 1987), 7th ed..
[24] H. Wagner, Z. Angew. Math. Mech. **12**, 193 (1932).
[25] A. Korobkin and V. V. Pukhnachov, Annu. Rev. Fluid Mech. **20**, 159 (1988).
[26] A. Mongruel, V. Daru, F. Feuillebois, and S. Tabakova, Phys. Fluids **21**, 032101 (2009).
[27] In [22] it is shown that the ejected flux per unit length of tangential momentum is proportional to $\rho V^2 Rs$, with Rs the radius of the impacting region. In the present case, $s = a(t)$.
[28] S. Howison, J. Ockendon, and S. Wilson, J. Fluid Mech. **222**, 215 (1991).
[29] J. M. Oliver, PhD. thesis, Oxford University, 2002.
[30] Y. Scolan and A. Korobkin, J. Fluids Struct. **17**, 275 (2003).
[31] F. MacIntyre, J. Geophys. Res. **77**, 5211 (1972).
[32] S. Gekle, J. M. Gordillo, D. van der Meer, and D. Lohse, Phys. Rev. Lett. **102**, 034502 (2009).
[33] S. Gekle and J. M. Gordillo, J. Fluid Mech. **663**, 293 (2010).
[34] A. Marchand, T. S. Chan, J. H. Snoeijer, and B. Andreotti, Phys. Rev. Lett. **108**, 204501 (2012).
[35] The value of α should be dependent on the wetting properties of the substrate but, in the case of our experiments, all the liquids partially wet the substrate with a similar contact angle $\sim 20°$.
[36] L. V. Zhang, J. Toole, K. Fezzaa, and R. Deegan, J. Fluid Mech. **703**, 402 (2012).